Article

Layered Copper Hydroxide Salts as Catalyst for the "Click" Reaction and Their Application in Methyl Orange Photocatalytic Discoloration

Rafael Marangoni [1,*]**, Rafael E. Carvalho** [1]**, Monielly V. Machado** [1]**, Vanessa B. Dos Santos** [2]**, Sumbal Saba** [3]**, Giancarlo V. Botessele** [1,*] **and Jamal Rafique** [2,3,*]

1   Departamento de Química (DEQ), Universidade Estadual do Centro-Oeste (UNICENTRO), Guarapuava 85040-167, PR, Brazil
2   Instituto de Química (INQUI), Universidade Federal do Mato Grosso do Sul (UFMS), Campo Grande 79074-460, MS, Brazil
3   Instituto de Química (IQ), Universidade Federal de Goiás (UFG), Goiânia 74690-900, GO, Brazil
*   Correspondence: rmarangoni@unicentro.br (R.M.); giancarlo@unicentro.br (G.V.B.); jamal.chm@gmail.com or jamal.rafique@ufms.br (J.R.)

Abstract: The 1,2,3-triazoles are an important class of organic compounds that are found in a variety of biologically active compounds. The most usual and efficient methodology to synthetize these compounds is the Copper-catalyzed Azide–Alkyne Cycloaddition (CuAAC), preferably by use of click chemistry principles. Therefore, the development of simple, robust, easily accessible and efficient materials as catalysts for this kind of reaction is highly desirable. In this sense, layered hydroxide salts (LHS) emerge as an interesting alternative for the click reaction. Thus, we describe herein the preparation and characterization of copper (II) layered hydroxide salts and their application as catalysts for the CuAAC reaction under solvent-free conditions. This synthetic methodology of CuAAC reaction is attractive as it follows several concepts of green chemistry, such as being easy to perform, allowing purification without chromatographic column, the process forming no sub-products, affording the desired 1,2,3-triazoles in the specific 1,4-disubstituted position in high yield, and having a short reaction time. Moreover, the photocatalysis for the degradation of methyl orange was also highly efficient using the same catalyst.

Keywords: layered hydroxide salts; copper (II) hydroxide acetate; copper (II) hydroxide nitrate; photocatalysis; methyl orange; click reaction; triazole

1. Introduction

In recent years, layered materials have attracted increasing attention in different areas of research. These structures are composed by the stacking of units known as layers, which have versatility of composition. The electrical nature of the layer of the material is used for their classification [1]. Thus, there are negatively charged layered compounds, neutral compounds, and positively charged compounds. For the last case, which are compounds that host anionic species in their interlamellar space, the main examples are the layered double hydroxides (LDH) and layered hydroxide salts (LHS) [2].

A wide range of applications of layered materials is available in the literature, as adsorbents [3], pigments [4,5], and drug carriers [6,7], among many other applications. Additionally, there are also reports of their use as catalysts [8,9]. As catalysts, the layered materials can be divided into three classes: layered structures where crystal anisotropy exists, multi-layer catalysts, and delaminated materials [10].

In the case of layered structures, with crystal anisotropy and layer positively charged, the LDH has the major contribution of uses and applications, and the LHS, despite these promising features, research with LHS has been relatively rare [11–13]. As far as their

chemical structure is concerned, LHS are similar to LDH, both being derived from brucite, $Mg(OH)_2$, but distinguishing themselves through the result of ion exchange processes. LDHs have an isomorphic substitution of divalent by trivalent metal ions, an LHS can be generally described under the formula $M^{2+}(OH)_{2-x}(A^{n-})_{x/n} \cdot yH^2O$, in which M^{2+} represents a divalent metal cation (e.g., Mg^{2+}, Ni^{2+}, Zn^{2+}, Cu^{2+}, etc.) and $A^{n-} \cdot yH_2O$ is a hydrated counter-ion (e.g., Cl^-, NO_3^-, SO_4^{2-}) that compensates for the excess of positive charge in the layers [12,14–16].

Furthermore, LHS compounds can be separated into two classes: in the first, the intercalated anions are free to move between the layers, while in the second, the anions bind covalently to the layers [17]. Layered hydroxide nitrates exemplify both the classes as mentioned earlier, as the zinc hydroxide nitrate ($Zn_5(OH)_8(NO_3)_2 \cdot 2H_2O$) has free nitrates between the layers and copper hydroxide nitrate ($Cu_2(OH)_3NO_3$) has nitrates bonded to the metal ions inside the layers [18].

Thus, the LSH has the predicates to be explored as catalysts or photocatalysts, like the LDH [19]. A variety of photocatalysts have been explored in recent decades, and some limitations in present photocatalytic systems can bring down their overall performance. The planar structure of layered materials endows them with abundant surface atoms and certainly provides sufficient space for integration with co-catalysts. This feature boosts the number of active sites for catalytic reactions, and more importantly, their reduced thickness offers the flexibility of enhancing catalytic activity by creating new active sites [19–21].

Among organic transformations, copper-catalyzed azide-alkyne cycloaddition (CuAAC), known as "click reaction", is a well-known protocol for the construction of triazoles [22,23]. Due to its efficiency and diversity in the suberates, Cu-AAC has been utilized to access sophisticated compounds with applications in diverse areas [24–27]. Considering the importance of Cu-AAC in the preparation of triazole, several copper-based materials have been used as catalysts [22,23,27].

In recent years, there has been an increasing trend toward minimizing the use of solvents, and various types of organic transformations have been carried out with the application of solvent-free conditions [28–32], making the synthesis greener.

To the best of our knowledge, the application of copper-containing LHS in photo-discoloration, as well as a catalyst in the CuAAC, has not yet been explored. Thus, in connection with our continuing interest in designing new materials [33,34] and transition metal-catalysis [35–38], as well as in developing eco-friendly processes for cross-coupling reactions [39–44], we herein report the synthesis and characterization of copper (II) layered hydroxide salts and their application as catalyst for the CuAAC reaction under solvent-free conditions. Furthermore, Cu-based LHS was also successfully applied in the photocatalytic degradation of methyl orange. The material with acetate ions showed better results than with nitrate ions for the click reactions. For photocatalysis, the LHS intercalated with nitrates proved to be more interesting than the material with acetate, as the catalyst does not have any structural changes.

2. Results and Discussion

2.1. Characterization of Catalysts

The prepared copper (II) layered hydroxide salts with acetate and nitrate intercalated were characterized, using X-ray diffraction (XRD), Fourier Transform Infrared Spectroscopy (FTIR), and Scanning Electron Microscopy (SEM) techniques.

2.1.1. X-ray Diffraction (XRD)

Figure 1 shows the X-ray diffraction analyses for the layered copper (II) hydroxide salts synthesized with intercalated acetate and nitrate.
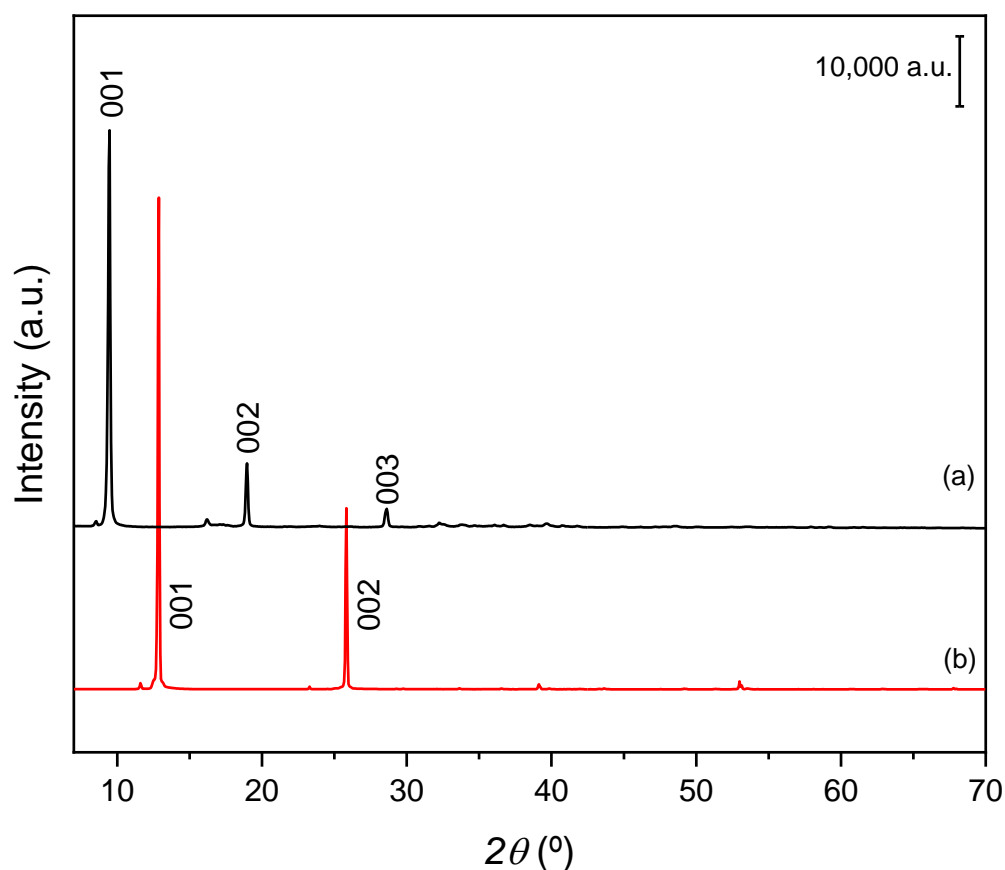
Figure 1. X-ray diffraction patterns of (a) copper hydroxy acetate and (b) copper hydroxy nitrate.

The copper hydroxide acetate shows a layered pattern of X-ray diffraction (Figure 1a), with basal plane diffraction peaks (001, 002 and 003) that correspond to an interplanar spacing of 9.91 Å [11,45]. For the copper (II) hydroxy nitrate (Figure 1b), the X-ray diffraction pattern agrees with a monoclinic phase, and the basal distance corresponds to 6.85 Å to peak 001, and its multiple 002 [46,47].

The other small peaks are attributed to the diffraction planes of the internal organization of the layers of the material. Both materials were synthesized with a crystalline phase distinct from that of the precursor salts, and the hydroxide salts obtained showed no peaks corresponding to copper (II) oxide and/or copper (II) hydroxide [47]. In fact, the X-ray patterns are consistent with copper (II) hydroxy acetate with the formula $Cu_2(OH)_3(OCOCH_3).H_2O$ formula and copper (II) hydroxy nitrate, with the formula $Cu_2(OH)_3NO_3$.

2.1.2. Fourier Transform Infrared Spectroscopy (FTIR)

Figure 2 shows the infrared analyses for the layered copper (II) hydroxide salts synthesized with intercalated acetate and nitrate.

The FTIR spectrum of $Cu_2(OH)_3(OCOCH_3)\cdot H_2O$ in the region from 3700 to 3000 cm^{-1} is attributed to OH-group vibrational modes and demonstrates a low presence of water molecules in the material. Low-intensity bands were observed at 3609, 3574, 3520, 3455, 3353 and 3237 cm^{-1}, and can be attributed to water and matrix hydroxide groups. The region between 1050 and 650 cm^{-1} is attributed to Cu-O-H bonds, and for copper hydroxide acetate were found bands at 649, 792, 1021 and 1046 cm^{-1}. The absorption bands of carboxyl groups were observed normally at 1549 cm^{-1}, attributed to asymmetric O-C=O, and 1409 cm^{-1}, attributed to symmetric O-C=O vibrations, and in the copper hydroxide acetate was seen at 1606, 1541, 1406, 1345 cm^{-1}. In the LHS, the two original bands were split into four bands after functionalization of acetate to the copper layer [11,46].
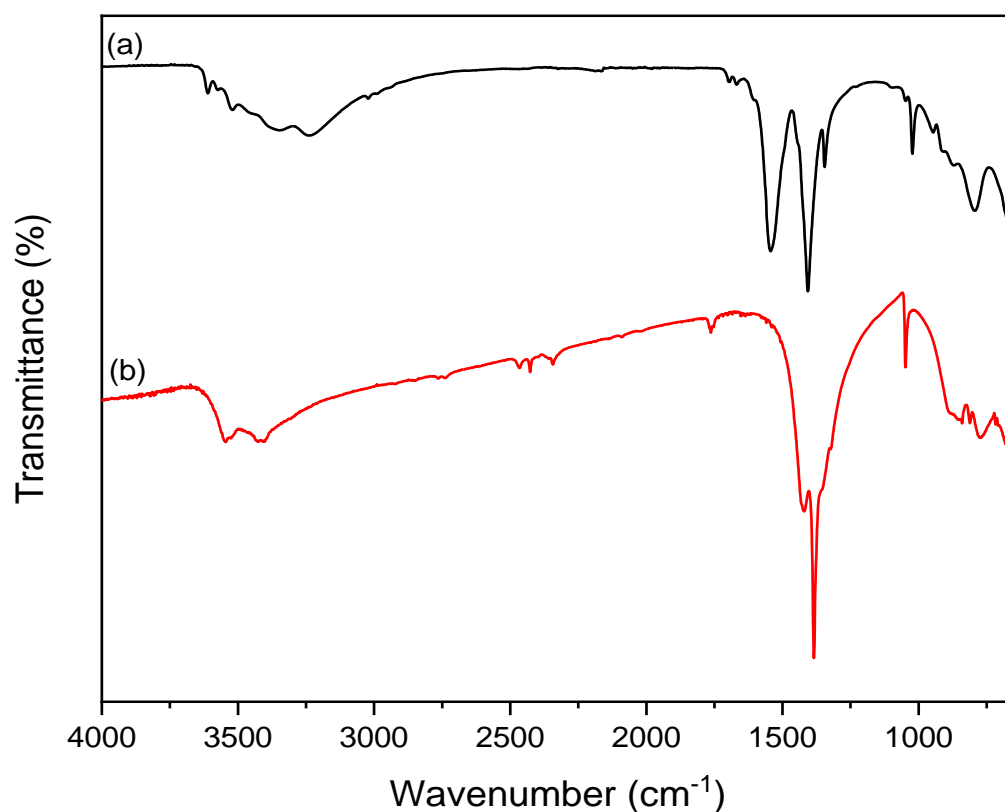
Figure 2. FTIR spectra of (a) copper hydroxy acetate and (b) copper hydroxy nitrate.

The IR spectrum of $Cu_2(OH)_3NO_3$ synthesized (Figure 2b) exhibited vibrational peaks observed at 3542 and 3412 cm^{-1}. These peaks cab be attributed to structural OH^- layers groups and water molecules in the interlayer space, respectively. The band centered at 3542 cm^{-1} corresponds to free OH groups, while the band at 3412 cm^{-1} indicates the presence of hydrogen-bonded OH groups. The nitrate (NO_3^-) peaks can be identified at 810, 1049, 1354 (a shoulder), 1383, and 1420 cm^{-1}, whose interaction with copper hydroxide layers is evidenced by the appearance of symmetric and asymmetric stretching modes of NO_3^- at 1420 and 1354. The band at 1049 cm^{-1} corresponds to the N-O stretching vibration of a monodentate O-NO group, in good agreement with the literature. The peak observed at 1383 cm^{-1} is also assigned to free nitrate ions in the interlayer space. The frequencies of the vibrational modes attributed to Cu-O-H bonds are dependent on the degree of hydrogen bonding and were found at 888, 773, and 675 cm^{-1}. The bands observed to the $Cu_2(OH)_3NO_3$ are in agreement with the literature [46,47].

2.1.3. Scanning Electron Microscopy (SEM)

SEM was used to portray the shape and size of the prepared copper layered hydroxide salts. The SEM images are shown in Figure 3, with different magnifications.

The $Cu_2(OH)_3(OCOCH_3)$ synthesized has its SEM images shown in Figure 1a,c,e, and this material forms thin round plate-like crystals. Other authors in the literature had normally reported a rectangular shape for the copper hydroxide acetate [45]. For the SEM images of the $Cu_2(OH)_3NO_3$ synthesized, the images show well-crystallized particles with well-defined 120° angles in a plate-like morphology (Figure 3b,d,f) [47,48]. The particles of the synthesized LHS show a considerable difference in particle size, where for the $Cu_2(OH)_3(OCOCH_3)$bserved particles with an average size of 10 μm, and for the $Cu_2(OH)_3NO_3$observed particles with a size range between 40–60 μm.

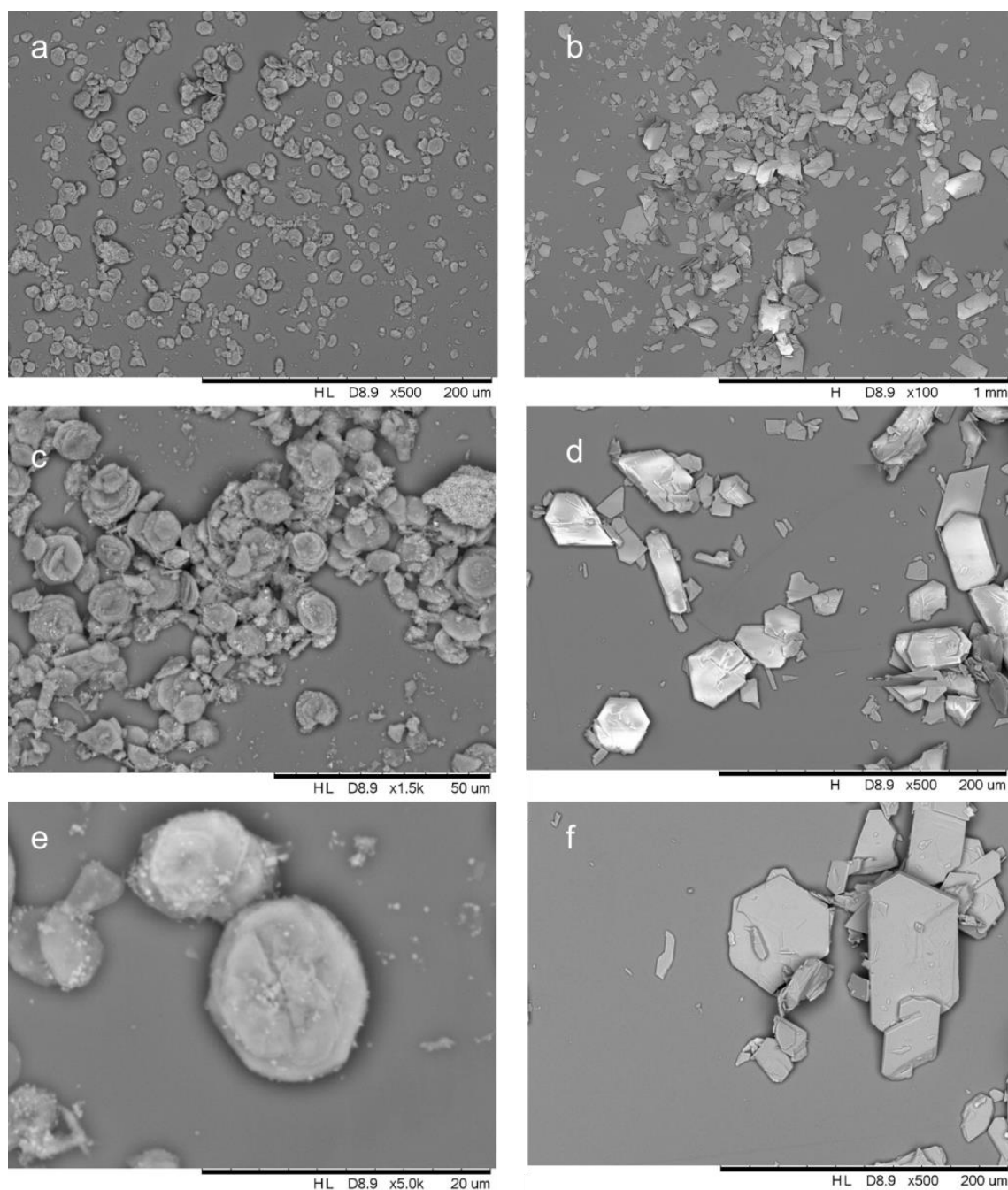**Figure 3.** SEM images of (**a**,**c**,**e**) copper hydroxy acetate, and (**b**,**d**,**f**) copper hydroxy nitrate, in different magnifications.

2.2. Evaluation of the Photocatalytic Activity of the LHS

Methyl orange (MO) is a common anionic dye that is harmful to the environment and biology, so it must be treated innocuously before it can be disposed of. MO was chosen as a model pollutant to study the performance of layered hydroxide salts as photocatalysts in the presence of UV/Vis light for the discoloration of dye before its disposal.

Figure 4 shows the UV-Vis spectra and the respective X-ray diffraction patterns after the photocatalysis reactions for the different reaction conditions for the $Cu_2(OH)_3(OCOCH_3)$ acting as photocatalyst.

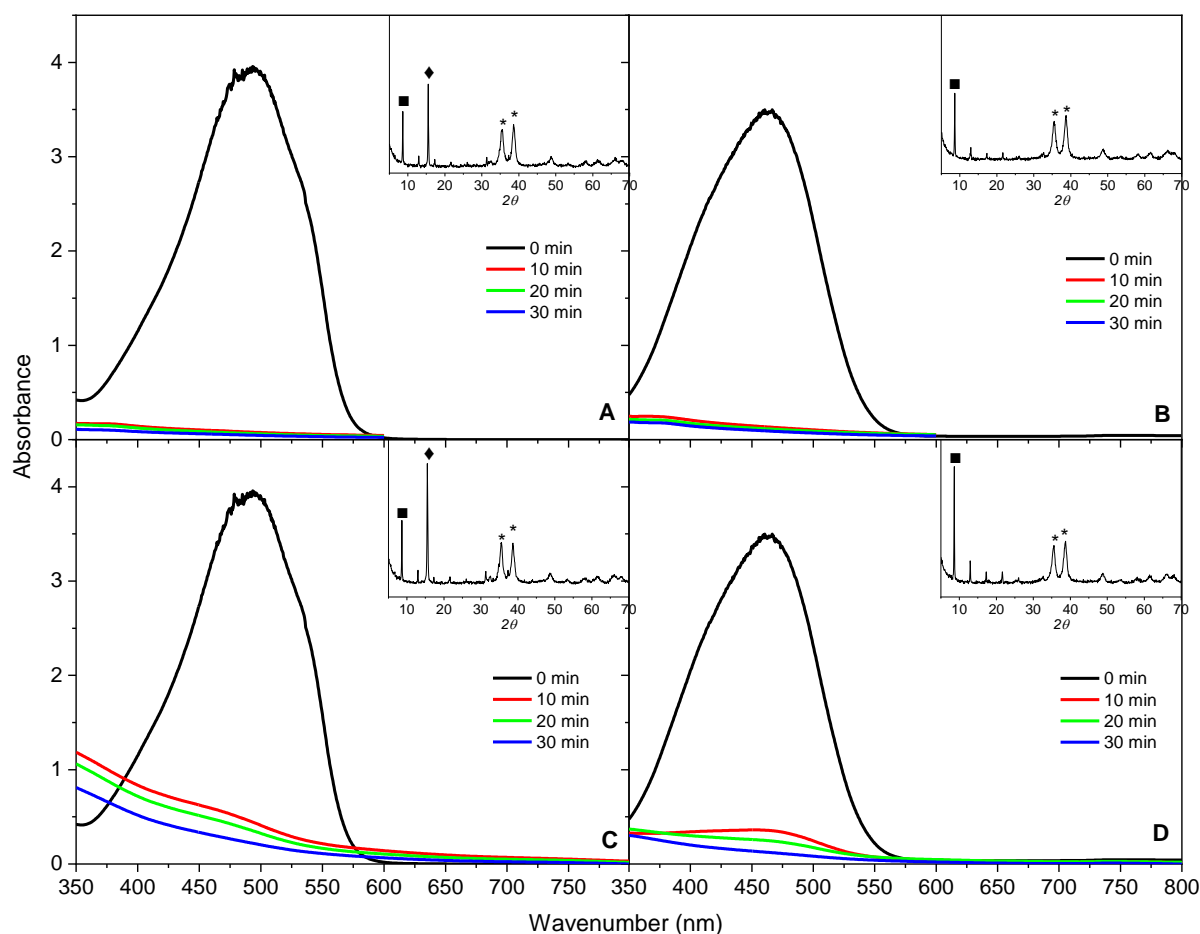**Figure 4.** UV-Vis spectra of methyl orange photocatalysis using the $Cu_2(OH)_3(OCOCH_3)$ as catalyst. The reaction conditions were: (**A**) pH 3 and temperature 25 °C, (**B**) pH 9 and temperature 25 °C, (**C**) pH 3 and temperature 50 °C, and (**D**) pH 9 and temperature 50 °C. The insets represent the X-ray diffraction pattern for each catalyst after the reaction.

After 10 min of testing, the reaction medium was practically translucent for the conditions where the temperature was set at 25 °C (Figure 4A,B), with solution discoloration rates as high as 97.75% (pH3/T25 °C) and 98.18% (pH9/T25 °C). These conditions showed a rapid rate of discolorization when compared to the tests carried out at 50 °C, where they had discolorization rates of 88.29% (pH3/T50 °C) and 89.77% (pH9/T50 °C) after the same 10-min reaction. After completion of the experiments in the tested reaction media, the discolorations (at 30 min) were observed, and the minimum value obtained was 94.20% for the pH3/T50 °C condition and a maximum of 98.66% for the pH3/T25 °C condition. For all cases, the solution was monitored at 465 nm. Table 1 compiles the results of the discolorations obtained for the $Cu_2(OH)_3(OCOCH_3)$ used as catalyst.

Table 1. Percentage of discoloration for each photocatalysis reaction using the $Cu_2(OH)_3(OCOCH_3)$ as catalyst.

pH	Temperature (°C)	Discoloration (%)		
		10 min	**20 min**	**30 min**
3	25	97.75	98.18	98.66
9	25	96.20	96.78	97.41
3	50	88.29	90.68	94.20
9	50	89.77	92.91	96.49

After the photocatalysis reactions, the catalysts were evaluated by X-ray diffraction technique, where for all cases, the catalyst was partially converted to copper (II) oxide (marked with * in the XRD of the insets of Figure 4), and another phase in which the methyl orange has intercalated into the LHS, presenting a basal distance of 20.59Å (indicated in the insets by ■), being coherent with the intercalation of the dye into the LHS. For the conditions tested at pH 3, a phase with a basal distance of 5.71 Å was still observed, which is mainly attributed to copper (II) hydroxide, marked with ◆.

Figure 5 shows the UV-Vis spectra and the respective X-ray diffraction patterns after the photocatalysis reactions for the different conditions of reaction for the $Cu_2(OH)_3(NO_3)$ acting as photocatalyst.

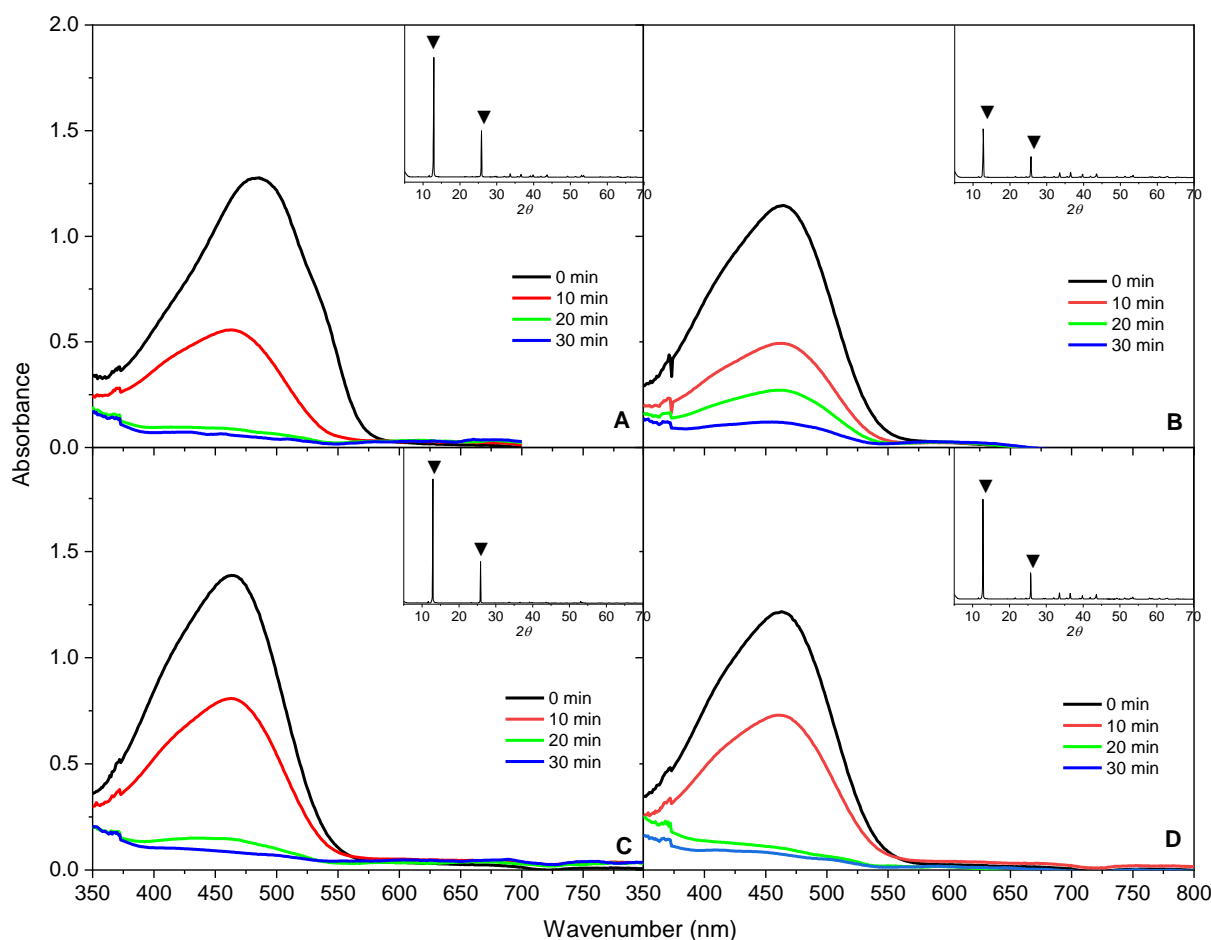**Figure 5.** UV-Vis spectra of methyl orange photocatalysis using the $Cu_2(OH)_3NO_3$ as catalyst. The reaction conditions were: (**A**) pH 3 and temperature 25 °C, (**B**) pH 9 and temperature 25 °C, (**C**) pH 3 and temperature 50 °C, and (**D**) pH 9 and temperature 50 °C. The insets represent the X-ray diffraction pattern for each catalyst after reaction.

By using a catalytic amount of $Cu_2(OH)_3NO_3$ LHS, after 30 min of photo-discoloration at under room temperature (25 °C), the catalyst removed 95.22% of methyl orange at pH 3 (Figure 5A), and 89.65% at pH 9 (Figure 5B). Contrary to LHS intercalated with acetate ions, LHS intercalated with the nitrate ion resulted in a slower discoloration (Table 2). After 10 min of reaction, around 41~56% was discolored.

Table 2. Percentage of discoloration for each photocatalysis reaction using the $Cu_2(OH)_3NO_3$ as catalyst.

pH	Temperature (°C)	Discoloration (%)		
		10 min	20 min	30 min
3	25	53.79	92.69	95.22
9	25	56.85	76.32	89.65
3	50	42.86	85.04	93.99
9	50	41.60	89.57	94.22

After the discoloration reactions, the $Cu_2(OH)_3NO_3$ (catalyst) was evaluated by X-ray diffraction. The patterns obtained can be seen in the insets of Figure 5, for the respective reaction conditions. In all cases, the $Cu_2(OH)_3NO_3$ structure remained unchanged after the photo-discoloration reactions of the methyl orange dye, showing only peaks referring to the pure phase of $Cu_2(OH)_3NO_3$ (marked with ▼). Although the solution's color removal efficiency is slightly lower than that observed for acetate-derived LHS, the catalyst does not undergo chemical and structural changes after the catalytic process.

A test was conducted in the absence of light to evaluate the influence of adsorption on the process. After 30 min of experiment, $Cu_2(OH)_3(OCOCH_3)$ removed 93%, and $Cu_2(OH)_3NO_3$ removed 5% of the methyl orange dye from the solution, and this discoloration is associated with an adsorption process. Figure 6 shows the UV-Vis spectra for the experiment in the absence of light.
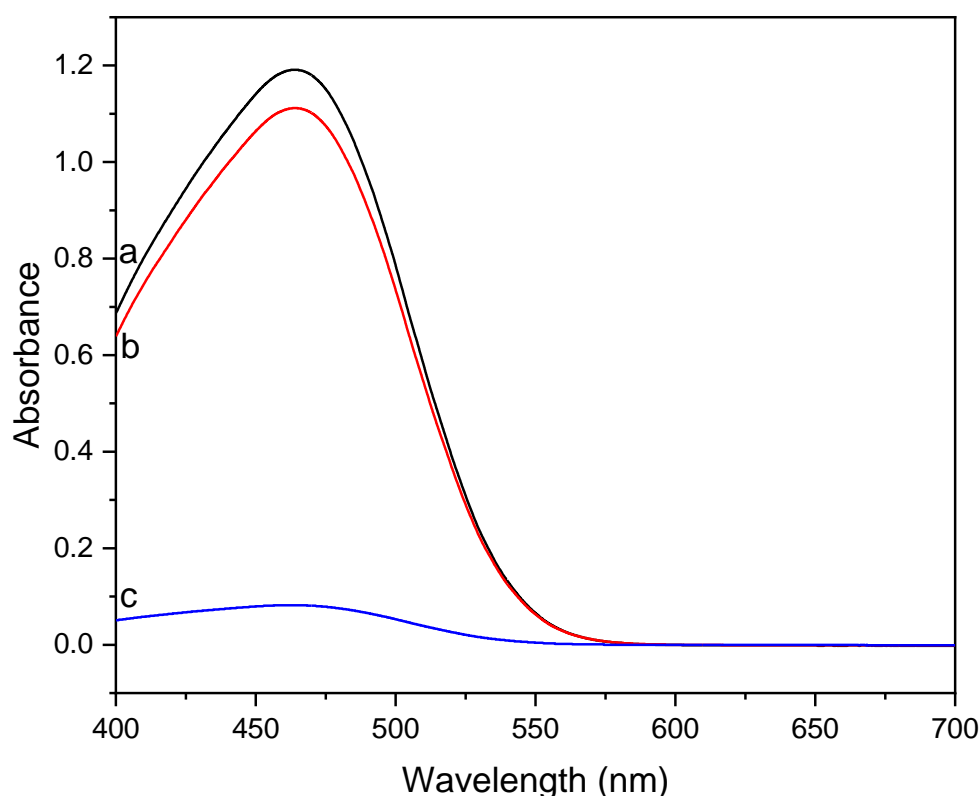
Figure 6. Experiment in the absence of light for a methyl orange solution (50 mg/L) at 0 min (a), and after 30 min for $Cu_2(OH)_3NO_3$ (b) and $Cu_2(OH)_3(CH_3COO)$ (c).
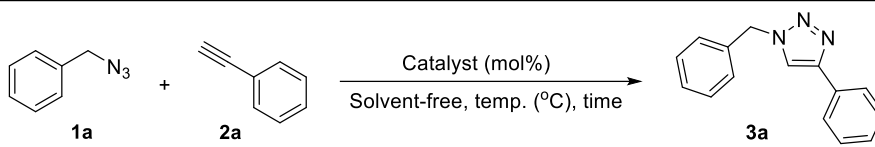
These results show that for $Cu_2(OH)_3(OCOCH_3)$, the observed values were due to adsorptive/photocatalytic process, while for $Cu_2(OH)_3NO_3$, the observed values were due to only the photocatalytic process, without the influence of adsorptive processes.

For this reason, acetate-derived LHS catalyst was analyzed after the photocatalytic process, in order to determine the amount of dye adsorbed over the catalyst. For this, the catalyst was isolated and digested in HCl. The digested solution was analyzed by UV-Vis to determine the amount of the dye. The result demonstrated that the quantity of the adsorbed dye amount was 23.75 mg/g, which indicated that the process for this catalyst is a concomitant process between adsorption and photocatalysis.

2.3. Click Reaction for the Synthesis of 1,4-Disubstituted-1,2,3-Triazoles

In order to check the applicability of copper (II) layered hydroxides salts ($Cu_2(OH)_2$-($OCOCH_3$)) as catalyst for the Copper-catalyzed Azide-Alkyne Cycloaddition (CuAAC), the click reaction was performed between the benzyl azide **1a** and phenyacetylene **2a** as model substrates to afford the 1,2,3-triazole **3a** under solvent-free reaction (Table 3).

Table 3. Optimization of standard reaction parameters [a].

Entry	Cat. (mol%)	T °C	Time (min)	Yield (%) [b]
1	$Cu_2(OH)_2(OCOCH_3)$ (5.0)	80	3	91
2	$Cu_2(OH)_2(OCOCH_3)$ (5.0)	70	5	87
3	$Cu_2(OH)_2(OCOCH_3)$ (5.0)	50	50	41
4	$Cu_2(OH)_2(OCOCH_3)$ (2.5)	80	3	93
5	$Cu_2(OH)_2(OCOCH_3)$ (1.0)	80	5	91
6	$Cu_2(OH)_3NO_3$ (2.5)	80	120	67

[a] Reaction conditions: benzyl azide **1a** (0.69 mmol), phenyacetylene **2a** (0.69 mmol) and catalyst. [b] Yield of isolated product.

Initially, the temperature and time (Table 3, entries 1–3) of the reaction was optimized by analysing consumption of the starting materials through thin-layer chromatography (TLC) plate or by precipitation of the product.

The best result was obtained at 80 °C with a reaction time of 3 min, affording the desired product **3a** in 91% yield, using 5 mol% of catalyst (Table 3, entry 1). Next, the catalyst loading from 1.0 to 5.0 mol% was evaluated (Table 3, entries 1, 4 and 5). To our delight, by decreasing the catalytic loading for 2.5 and 1.0 mol%, respectively, there was no significant change in the yield, and when using only 1.0 mol% of catalyst, the product was precipitated in just 5 min, in 91% yield (Table 3, entry 5). Furthermore, the CuAAC reaction was also performed with $Cu_2(OH)_3NO_3$ as catalyst (Table 3, entry 6). However, after 120 min of reaction, the product **3a** was obtained in only 66% yield. This catalytic difference of the two hydroxysalts may be due the smaller interlamellar space of $Cu_2(OH)_3NO_3$ when compared with $Cu_2(OH)_2(OCOCH_3)$, which makes interactions with the copper catalytic site more difficult.

With best reaction conditions in hand (Table 3, entry 5), the scope of the click reaction was evaluated (Table 4). The methodology resulted in excellent yields when used in electron donating groups (Me and OMe) at the aromatic ring of acetylene (**2b** and **2c**), affording the 1,4-disubstituted-1,2,3-triazole **3b** and **3c** in 90 and 95% yield, respectively (Table 4, entries 2 and 3). 4-Ethynylaniline **2d** also tolerated this methodology, furnishing the product **3d** in 75% yield (Table 4, entry 4). Moreover, 2-ethynylnaphthalene **2e** reacted very well with benzyl azide **1a** to afford the 1,2,3-triazole **3e** in 86% yield (Table 4, entry 5).

Table 4. Synthesis of Cu$_2$(OH)$_2$(OCOCH$_3$)-catalyzed 1,4-disubstituted-1,2,3-triazoles [a].

Entry	Acetylene	Product	Yield (%) [b]
1	**2a**	**3b**	91
2	**2b**	**3b**	90
3	**2c**	**3c**	95
4	**2d**	**3c**	75
5	**2e**	**3e**	86

[a] Reaction conditions: benzyl azide **1a** (0.69 mmol), acetylene **2a–e** (0.69 mmol), Cu$_2$(OH)$_2$(OCOCH$_3$) (1.0 mol%), 80 °C, solvent-free. [b] Yield of isolated product.

2.4. Recyclability of the Catalyst

In order to check the efficiency of the catalyst, a recyclability test was performed (Table 5). After the first run, the reaction mixture was washed with ethyl acetate (4 × 20 mL) to recover the catalyst. The recovered catalyst was air-dried at room temperature (for a period of 12 h), without any further treatment. The resulting dried materials were reused as catalyst for three reaction cycles, by using benzyl azide **1a** and phenylaetylene **2a**, under the standard conditions. In all these cycles, the desired product **3a** was obtained in 80–90% yields (Table 5).

Table 5. Catalyst recycling [a].

Cycle	Yield (%) [b]
1	91
2	90
3	88
4	80

[a] Reaction conditions: benzyl azide **1a** (4.0 mmol), acetylene **2a** (4.0 mmol), Cu$_2$(OH)$_2$(OCOCH$_3$) (1.0 mol%), 80 °C, solvent-free. [b] Yield of isolated product.

Figure 7 shows the X-ray diffraction pattern for the LHS after the recyclability tests. After the third recycle test, the catalyst changed its structure, where part of the material was converted to copper oxide (marked with *). A phase with a basal distance of 5.44Å corresponding to copper (II) hydroxide (marked with ◆) was also observed, and a peak at lower angles indicated intercalation of the reactant molecules in the interlamellar space of the catalyst, with a basal distance of 15.27Å (●).
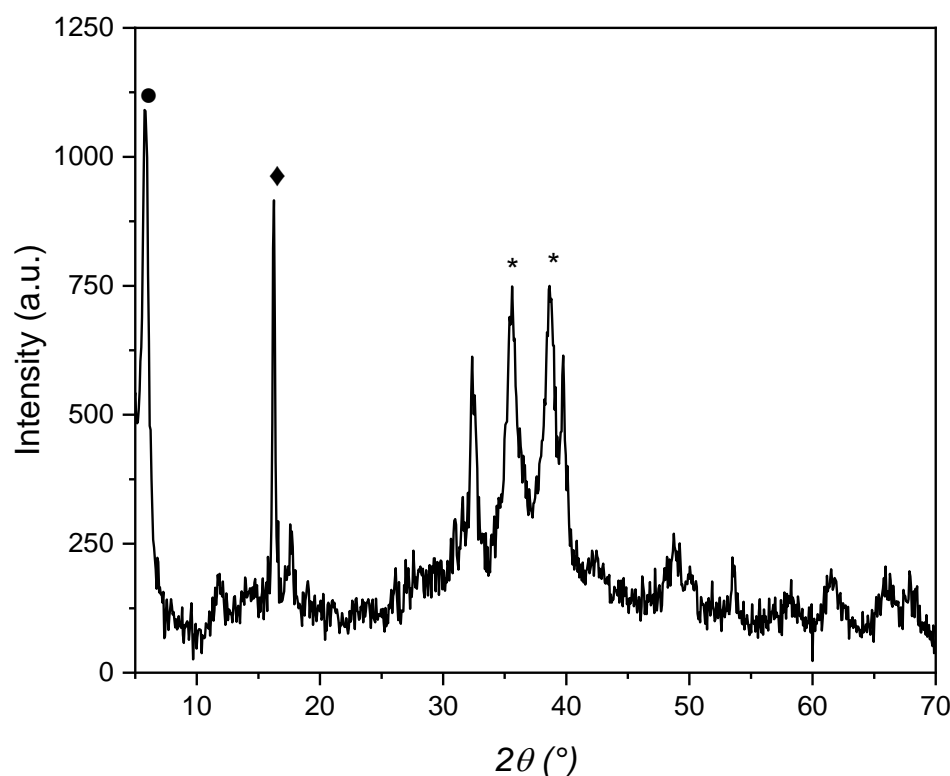
Figure 7. X-ray diffraction pattern of copper hydroxy acetate after the third recycle test.

3. Materials and Methods

3.1. General Information

All starting materials, reagents, and solvents were commercially available. Thin-layer chromatography (TLC) was performed using Macherey-Nagel GF254, 0.20 mm thickness. For the visualization, TLC plates were placed under UV light (254 nm), stained with iodine vapour, and developed with sulfuric vanillin burned. ^{1}H and ^{13}C NMR spectra were taken on a Bruker DPX-300 Avance spectrometer, with CDCl$_3$. As noted, ^{1}H NMR spectra were referenced to 0.00 ppm (TMS), and ^{13}C NMR spectra were referenced to 77.16 ppm (CDCl$_3$). All chemical shifts are reported in parts per million (ppm), and coupling constants (*J*) are expressed in Hertz (Hz).

3.2. Copper (II) Layered Hydroxide Salts Synthesis

The synthesis method used was the salt-base method, as described in the literature [11,45], where a salt solution was prepared with the copper (II) salt, in this case, the copper acetate II monohydrate, dissolving it in distilled water in a beaker. Then, a previously prepared sodium hydroxide solution (NaOH, 0,1 molL^{-1}) was added slowly, drop by drop, to the copper (II) acetate solution, with constant vigorous stirring, to reach a pH of 8. The resulting greenish-blue solid with formulation of Cu$_2$(OH)$_3$(OCOCH$_3$). H$_2$O was centrifuged at 3500 rpm, washed with water (five times), and dried at 80 °C for 24 h.

For the Cu$_2$(OH)$_3$NO$_3$ synthesis the same method was used as described for the previous LHS, using copper (II) nitrate as the starting salt of the reaction. The bluish-green material obtained was centrifuged at 3500 rpm, washed with water (five times), and dried at 80 °C for 24 h.

3.3. Evaluation of the Photocatalytic Activity of the LHS

The evaluation of the photocatalytic reaction was carried out inside a discontinuous reactor (as adapted from literature [49]), refrigerated with a thermostat (Nova Ética), containing 200 mL of aqueous solution of the methyl orange (50 mgL^{-1}) used as substrate of interest and 350 mg of LHS as catalyst. The substrate was irradiated using a 125 W mercury

vapor lamp (without the original glass bulb), inserted into the solution through a quartz bulb (UVC radiation). The experiments were performed at pH 3 or 9, the temperature stabilized at 25 or 50 °C, and the reaction time was 30 min, evaluating 3 mL aliquots every 10 min at the maximum wavelength observed in UV-Vis spectroscopy for methyl orange. The discoloration rate (%) of methyl orange was calculated by using the equation:

$$DR\% = \frac{C_0 - C_t}{C_0} \times 100$$

where DR is the discoloration rate (%), C_0 is the initial concentration of MO, and C_t is the concentration of MO after 10, 20, or 30 min [50].

An additional experiment was performed in the absence of light to evaluate the influence of adsorption on the process. The temperature was controlled with a thermostat bath at 25 °C, under stirring, for 30 min. After this period, the solution was monitored using UV-Vis spectroscopy.

3.4. General Procedure for the Synthesis of 1,4-Disubstituted-1,2,3-Triazoles

In a 5 mL tube, was added benzyl azide (0.69 mmol, 86 μL), acetylene (0.69 mmol) and $Cu_2(OH)_2(OCOCH_3)$ (1.0 mol%) under constant stirring and heating to 80 °C for 5 min. The product formation was monitored by TLC or by precipitation of the 1,2,3-triazole. When the reaction was complete, the product was extracted with diiodomethane and centrifuged three times (5 min, 3500 rpm). Then, the supernatant was separated and the solvent removed by reduced pressure, affording the desired products without the need for column chromatography.

(1) *1-benzyl-4-phenyl-1H-1,2,3-triazole (3a)* Supplementary Materials ^{1}H NMR (CDCl$_3$, 300 MHz): δ (ppm) = 7.67 (d, J = 7.8 Hz, 2H), 7.56 (s, 1H), 7.27–7.14 (m, 8H), 5.39 (s, 2H). ^{13}C NMR (CDCl$_3$, 75 MHz): δ (ppm) = 148.1; 134.7, 130.6, 129.1, 128.8, 128.7, 128.1, 128.0, 125.7, 119.7, 54.1.

(2) *1-benzyl-4-(p-tolyl)-1H-1,2,3-triazole (3b)* Supplementary Materials ^{1}H NMR (CDCl$_3$, 300 MHz): δ (ppm) = 7.69 (d, J = 8.0 Hz, 2H), 7.62 (s, 1H), 7.38–7.29 (m, 5H), 7.19 (d, J = 8.0 Hz, 2H); 5.54 (s, 2H); 2.35 (s, 3H). ^{13}C NMR (75 MHz, CDCl$_3$): δ (ppm) = 138.1, 134.9, 129.6, 129.2, 128.8, 128.1, 127.8, 125.7, 119.3, 54.3, 21.3.

(3) *1-benzyl-4-(4-methoxyphenyl) -1H-1,2,3-triazole (3c)* Supplementary Materials ^{1}H NMR (CDCl$_3$, 300 MHz): δ (ppm) = 7.71 (d, J = 8.8 Hz, 2H), 7.59 (s, 1H), 7.36–7.27 (m, 5H), 6.91 (d, J = 8.8 Hz, 2H), 5.52 (s, 2H), 3.80 (s, 3H). ^{13}C NMR (75 MHz, CDCl$_3$): δ (ppm) = 159.6, 134.8, 129.1, 128.7, 128.0, 127.0, 123.3, 118.9, 114.2, 55.3, 54.2.

(4) *4-(1-benzyl-1H-1,2,3-triazol-4-yl)aniline (3d)* Supplementary Materials ^{1}H NMR (CDCl$_3$, 300 MHz): δ (ppm) = 7.59 (d, J = 8.4 Hz, 2H), 7.52 (s, 1H), 7.36–7.26 (m, 5H); 6.70 (d, J = 8.4 Hz, 2H), 5.54 (s, 2H); 3.73 (br, 2H). ^{13}C NMR (75 MHz, CDCl$_3$): δ (ppm) = 141.3, 135.0, 129.2, 128.8, 128.2, 127.0, 121.3, 118.4, 115.5, 54.3.

(5) *1-benzyl-4-(naphthalen-2-yl)-1H-1,2,3-triazole (3e)* Supplementary Materials ^{1}H NMR (CDCl$_3$, 300 MHz): δ (ppm) = 7.89 (d, J = 8.4 Hz, 2H), 7.72 (s,1H), 7.67–7.63 (m, 4H); 7.48–7.35 (m, 6H); 5.61 (s, 2H). ^{13}C NMR (75 MHz, CDCl$_3$): δ (ppm) = 141.2, 140.7, 129.3, 129.0, 128.2, 127.6, 127.1, 126.2, 119.6, 54.4.

The ^{1}H and ^{13}C NMR spectra of all products are available in Support Information.

3.5. Material Characterization

The materials structure was studied with X-ray powder diffraction measurements performed in a Bruker Diffractometer, D2 Phaser, using Cu Kα radiation source (λ = 1.5418 Å), operating at 30 mA and 40 kV, range of 3 to 70° 2θ, and a dwell time of 0.05 °min^{-1}.

Infrared spectra with Fourier transform (FTIR) were collected with a PerkinElmer Frontier spectrophotometer, in the range of 4000–400 cm^{-1}, with resolution of 4 cm^{-1} and an accumulation of 32 scans. The analyses were performed using KBr tablets containing 1 wt% of the LHS.

The scanning electron microscopy (SEM) images were obtained using the Hitachi TM-3000 scanning electron microscope, operating in analytical mode at 15 kV.

The Ultraviolet-Visible spectra were obtained with a Shimadzu spectrophotometer, model UV-1800, operating in the range of 350–800 nm, using a 1 cm quartz path length cell.

4. Conclusions

In conclusion, we described herein the catalytic activity of copper (II) layered hydroxides salts (LHS) in the copper-catalyzed azide–alkyne cycloaddition (CuAAC) and in the photodecomposition of methyl orange dye. This simple methodology allowed the click reaction under solvent-free conditions, to afford selectively the 1,4,-dissubstituted-1,2,3-triazoles in high yields. Furthermore, the catalysts enabled a high rate of discoloration of the harmful dye after only 10 min of photocatalysis and reached discoloration rates above 90% within 30 min of reaction at room temperature.

The key features of this benign LHS-catalyzed protocol are: (1) ease to perform, purification without chromatographic column; (2) no formation of by-products; (3) selective formation of the desired products; (4) short reaction time; and (5) solvent-free reaction conditions.

Supplementary Materials: The following supporting information can be downloaded at: https://www.mdpi.com/article/10.3390/catal13020426/s1, ^{1}H and ^{13}C NMR spectra for all compounds.

Author Contributions: Conceptualization, R.M., G.V.B. and J.R.; synthesis, spectral analysis, characterizations, and reagents/materials, R.E.C., M.V.M., V.B.D.S. and S.S.; photocatalysis experiments, R.E.C. and M.V.M.; organic synthesis, R.E.C., V.B.D.S., S.S., G.V.B. and J.R.; writing—original draft, R.M., G.V.B. and J.R.; writing—review and editing, R.M., G.V.B. and J.R.; writing of the paper, R.M., G.V.B. and J.R. All authors have read and agreed to the published version of the manuscript.

Data Availability Statement: The data of this study is available on request from the corresponding author.

Conflicts of Interest: The authors declare no conflict of interest.

References

1. Silva, M.L.N.; Marangoni, R.; Cursino, A.C.T.; Schreiner, W.H.; Wypych, F. Colorful and transparent poly(vinyl alcohol) composite films filled with layered zinc hydroxide salts, intercalated with anionic orange azo dyes (methyl orange and orange II). *Mater. Chem. Phys.* **2012**, *134*, 392–398. [CrossRef]
2. Bravo-Suarez, J.; Paez-Mozo, E.A.; Oyama, S.T. Review of the synthesis of layered double hydroxides: A thermodynamic approach. *Quím. Nova* **2004**, *27*, 601–614. [CrossRef]
3. Jaerger, S.; Nogueira, D.A.D.; de Oliveira, D.S.; Machado, M.V.; Marangoni, R. Study of different morphology of zinc hydroxide salt as adsorbent of azo dyes. *ChemistrySelect* **2021**, *6*, 4354–4367. [CrossRef]
4. Silva, M.L.N.; Marangoni, R.; da Silva, A.H.; Wypych, F.; Schreiner, W.H. Poly(vinyl alcohol) composites containing layered hydroxide salts, intercalated with anionic azo dyes (Tropaeolin 0 and Tropaeolin 0). *Polímeros* **2013**, *23*, 248–256.
5. Marzec, A.; Szadkowski, B.; Rogowski, J.; Maniukiewicz, W.; Kozanecki, M.; Moszynski, D.; Zaborski, M. Characterization and properties of new color-tunable hybrid pigments based on layered double hydroxides (LDH) and 1,2-dihydroxyanthraquinone dye. *J. Ind. Eng. Chem.* **2019**, *70*, 427–438. [CrossRef]
6. Karmakar, A.K.; Hasan, M.S.; Sreemani, A.; Das Jayanta, A.; Hasan, M.M.; Tithe, N.A.; Biswas, P. A review on the current progress of layered double hydroxide application in biomedical sectors. *Eur. Phys. J. Plus* **2022**, *137*, 801. [CrossRef]
7. da Rocha, M.C.; Galdino, T.; Trigueiro, P.; Honorio, L.M.C.; Barbosa, R.D.; Carrasco, S.M.; Silva, E.C.; Osajima, J.A.; Viseras, C. Clays as vehicles for drug photostability. *Pharmaceutics* **2022**, *14*, 796. [CrossRef]
8. Cordeiro, C.S.; da Silva, F.R.; Marangoni, R.; Wypych, F.; Ramos, L.P. LDHs instability in esterification reactions and their conversion to catalytically active layered carboxylates. *Catal. Lett.* **2012**, *142*, 763–770. [CrossRef]
9. Gardona, Y.; Wegrzyn, A.; Miskowiec, P.; Korili, S.A.; Gil, A. Catalytic photodegradation of organic compounds using TiO2/pillared clays synthesized using a nonconventional aluminum source. *Chem. Eng. J.* **2022**, *446*, 136908. [CrossRef]
10. Centi, G.; Perathoner, S. Catalysis by layered materials: A review. *Microporous Mesoporous Mater.* **2008**, *107*, 3–15. [CrossRef]

11.　Marangoni, R.; Bubniak, G.A.; Cantão, M.P.; Abbate, M.; Schreiner, W.H.; Wypych, F. Modification of the interlayer surface of layered copper(II) hydroxide acetate with benzoate groups: Submicrometer fiber generation. *J. Colloid Interface Sci.* **2001**, *240*, 245–251. [CrossRef] [PubMed]

12.　Pan, B.; Li, J.; Xu, J.; Ma, J.; Liu, L.; Zhang, X.; Zhang, D.; Tong, Z. A novel hybrid constructed by the fabrication of exfoliated Cu-LHs nanosheets and MnTSPP anions. *Chem. Lett.* **2016**, *46*, 1–2. [CrossRef]

13.　Giraldo-Lodoño, C.C.; Ocampo-Cardona, R.; Ríos-Vásquez, L.A.; Martínez-Garzón, M.M.; Aguirre-Cortés, J.M. Palladium nanoparticles supported in laminar hydroxide salts: Potential use in Sonogashira reactions. *Rev. Colomb. Quim.* **2017**, *46*, 51–65. [CrossRef]

14.　Cursino, A.C.T.; Rives, V.; Arizaga, G.G.C.; Trujillano, R.; Wypych, F. Rare earth and zinc layered hydroxide salts intercalated with the 2-aminobenzoate anion as organic luminescent sensitizer. *Mater. Res. Bull.* **2015**, *70*, 336–342. [CrossRef]

15.　Caio, T.N.; Golçalves, N.; Wypych, F.; Lona, L.M.F. Enhancement of mechanical and thermal properties of poly(L-lactide) nanocomposites filled with synthetic layered compounds. *Int. J. Polym. Sci.* **2017**, *2017*, 1985078.

16.　Vasti, C.; Giacomelli, C.E.; Rojas, R. Pros and cons of coating layered double hydroxide nanoparticles with polyacrylate. *Appl. Clay Sci.* **2019**, *172*, 11–18. [CrossRef]

17.　Cursino, A.C.T.; Rives, V.; Carlos, L.D.; Rocha, J.; Wypych, F. layered zinc hydroxide salts intercalated with anionic surfactants and adsolubilized with UV absorbing organic molecules. *J. Braz. Chem. Soc.* **2015**, *26*, 1769–1780. [CrossRef]

18.　Rocha, M.G.; Nakagaki, S.; Ucoski, G.M.; Wypych, F.; Machado, G.S. Comparison between catalytic activities of two zinc layered hydroxide salts in brilliant green organic dye bleaching. *J. Colloid Interface Sci.* **2019**, *541*, 425–433. [CrossRef] [PubMed]

19.　Al-Soihi, A.S.; Alsulami, Q.A.; Mostafa, M.M.M. Amalgamated titanium oxide-carbon hollow sphere/nickel-layered double hydroxide as an efficient photocatalyst for the degradation of methyl orange. *Catalysts* **2022**, *12*, 1200. [CrossRef]

20.　Tan, C.; Cao, X.; Wu, X.-J.; He, Q.; Yang, J.; Zhang, X.; Chen, J.; Zhao, W.; Han, S.; Nam, G.-H. Recent advances in ultrathin two-dimensional nanomaterials. *Chem. Rev.* **2017**, *117*, 6225–6331. [CrossRef]

21.　Li, Y.; Gao, C.; Long, R.; Xiong, Y. Photocatalyst design based on two-dimensional materials. *Mater. Today* **2019**, *11*, 197–216. [CrossRef]

22.　Ladomenou, K.; Nikolaou, V.; Charalambidis, G.; Coutsolelos, A.G. "Click"-reaction: An alternative tool for new architectures of porphyrin based derivatives. *Coord. Chem. Rev.* **2016**, *306*, 1–42. [CrossRef]

23.　Wang, C.; Ikhlef, D.; Kahlal, S.; Saillard, J.-Y.; Astruc, D. Metal-catalyzed azide-alkyne "click" reactions: Mechanistic overview and recent trends. *Coord. Chem. Rev.* **2016**, *316*, 1–20. [CrossRef]

24.　Braga, F.C.; Ojeda, M.; Perdomo, R.T.; de Albuquerque, S.; Rafique, J.; Lime, D.P.; Beatriz, A. Synthesis of cardanol-based 1, 2, 3-triazoles as potential green agents against neoplastic cells. *Sustain. Chem. Pharm.* **2021**, *20*, 100408. [CrossRef]

25.　Blinder, W.H.; Sachsenhofer, R. 'Click' chemistry in polymer and materials science. *Macromol. Rapid Commun.* **2007**, *28*, 15–54. [CrossRef]

26.　France, M.S.; Saba, S.; Rafique, J.; Braga, A.L. KIO_4-mediated selective hydroxymethylation/methylenation of imidazo-heteroarenes: A greener approach. *Angew. Chem. Int. Ed.* **2021**, *60*, 18454–18460, reprinted in *Angew. Chem.* **2021**, *133*, 18602–18608. [CrossRef] [PubMed]

27.　Pasini, D. The Click Reaction as an efficient tool for the construction of macrocyclic structures. *Molecules* **2013**, *18*, 9512–9530. [CrossRef]

28.　Godoi, M.; Botteselle, G.V.; Rafique, J.; Rocha, M.S.T.; Pena, J.M.; Braga, A.L. Solvent-free fmoc protection of amines under microwave irradiation. *Asian J. Org. Chem.* **2013**, *2*, 746–749. [CrossRef]

29.　Tanaka, K.; Toda, F. Solvent-free organic synthesis. *Chem. Rev.* **2000**, *100*, 1025–1074. [CrossRef]

30.　Godoi, M.; Leitemberger, A.; Bohs, L.M.; Silveira, M.V.; Rafique, J.; D'Oca, M.G.M. Rice straw ash extract, an efficient solvent for regioselective hydrothiolation of alkynes. *Environ. Chem. Lett.* **2019**, *17*, 1441–1446. [CrossRef]

31.　Traboni, S.; Bedini, E.; Vessalla, G.; Iadonisi, A. Solvent-free approaches in carbohydrate synthetic chemistry: Role of catalysis in reactivity and selectivity. *Catalysts* **2022**, *10*, 1142. [CrossRef]

32.　Gawande, M.B.; Bonifacaio, V.D.B.; Luque, R.; Branco, P.S.; Varma, R.S. Solvent-free and catalysts-free chemistry: A benign pathway to sustainability. *ChemSusChem* **2013**, *7*, 24–44. [CrossRef]

33.　Scheide, M.R.; Petrele, M.M.; Neto, J.S.S.; Lenz, G.F.; Cezar, R.D.; Felix, J.F.; Botteselle, G.V.; Schneider, R.; Rafique, J.; Braga, A.L. Borophosphate glass as an active media for CuO nanoparticle growth: An efficient catalyst for selenylation of oxadiazoles and application in redox reactions. *Sci. Rep.* **2020**, *10*, 15233. [CrossRef] [PubMed]

34.　Matzkeit, Y.H.; Tornquist, B.L.; Manarin, F.; Botteselle, G.V.; Rafique, J.; Saba, S.; Braga, A.L.; Felix, J.F.; Schneider, R. Borophosphate glasses: Synthesis, characterization and application as catalyst for bis (indolyl) methanes synthesis under greener conditions. *J. Non-Cryst. Solids* **2018**, *498*, 153–159. [CrossRef]

35.　Tornquist, B.L.; Bueno, G.P.; Willig, J.C.M.; Oliveira, I.M.; Stefani, H.A.; Rafique, J.; Saba, S.; Iglesias, B.A.; Botteselle, G.V.; Manarin, F. Ytterbium (III) Triflate/Sodium Dodecyl Sulfate: A versatile recyclable and water-tolerant catalyst for the synthesis of Bis (Indolyl) Methanes (Bims). *ChemistrySelect* **2018**, *3*, 6358–6363. [CrossRef]

36.　Peterle, M.M.; Scheide, M.R.; Silva, L.T.; Saba, S.; Rafique, J.; Braga, A.L. Copper-catalyzed three-component reaction of oxadiazoles, elemental Se/S and aryl iodides: Synthesis of chalcogenyl (Se/S)-oxadiazoles. *ChemistrySelect* **2018**, *3*, 13191–13196. [CrossRef]

37. Rocha, M.S.T.; Rafique, J.; Saba, S.; Azeredo, J.B.; Back, D.; Godoi, M.; Braga, A.L. Regioselective hydrothiolation of terminal acetylene catalyzed by magnetite (Fe$_3$O$_4$) nanoparticles. *Synth. Commun.* **2017**, *47*, 291–298. [CrossRef]

38. Saba, S.; Santos, C.R.; Zavarise, B.R.; Naujorks, A.A.S.; France, M.S.; Schnedier, A.R.; Scheide, M.R.; Affeldt, R.F.; Rafique, J.; Braga, A.L. Photoinduced, direct C(sp^2)−H bond azo coupling of imidazoheteroarenes and imidazoanilines with aryl diazonium salts catalyzed by eosin Y. *Chem. Eur. J.* **2020**, *26*, 4461–4466. [CrossRef] [PubMed]

39. Rafique, J.; Saba, S.; Franco, M.S.; Bettanin, L.; Schneider, A.R.; Silva, L.T.; Braga, A.L. Direct, metal-free C (sp^2)-H chalcogenation of indoles and imidazopyridines with dichalcogenides, catalysed by KIO$_3$. *Chem. Eur. J.* **2018**, *24*, 4173–4180. [CrossRef]

40. Saba, S.; Rafique, J.; Braga, A.L. Synthesis of unsymmetrical diorganyl chalcogenides under greener conditions: Use of an iodine/DMSO system, solvent-and metal-free approach. *Adv. Synth. Catal.* **2015**, *357*, 1446–1452. [CrossRef]

41. Rafique, J.; Saba, S.; Frizon, T.E.A.; Braga, A.L. Fe$_3$O$_4$ nanoparticles: A robust and magnetically recoverable catalyst for direct C-H bond selenylation and sulfenylation of benzothiazoles. *ChemistrySelect* **2018**, *3*, 328–334. [CrossRef]

42. Botteselle, G.; Elias, W.C.; Bettanin, L.; Canto, R.F.S.; Salin, D.N.; Barbosa, F.A.R.; Saba, S.; Gallardo, H.; Ciancalenoi, G.; Domingos, J.B.; et al. Catalytic antioxidant activity of bis-aniline-derived diselenides as GPx mimics. *Molecules* **2021**, *26*, 4446. [CrossRef] [PubMed]

43. Meirinho, A.G.; Pereira, V.F.; Martins, G.M.; Saba, S.; Rafique, J.; Braga, A.L.; Mendes, S.R. Electrochemical oxidative C(sp^2)–H Bond selenylation of activated arenes. *Eur. J. Org. Chem.* **2019**, *38*, 6465–6469. [CrossRef]

44. Doerner, C.V.; Scheide, M.R.; Nicoleti, C.R.; Durigon, D.C.; Idiarte, V.D.; Sousa, M.J.A.; Mendes, S.R.; Saba, S.; Neto, J.S.S.; Martins, G.M.; et al. Versatile electrochemical synthesis of selenylbenzo [*b*] furans derivatives through the cyclization of 2-alkynylphenols. *Front Chem.* **2022**, *10*, 880099. [CrossRef]

45. Naofumi, K.; Hisayoshi, M.; Hiroyasu, F.; Fumitaka, E.; Komarneni, S. Synthesis and characterization of copper hydroxide acetate with a layered discoid crystal. *J. Mater. Res.* **2005**, *20*, 328–334.

46. Pereira, D.C.; de Faria, D.L.A.; Constantino, V.R.L. Cu^{II} Hydroxy Salts: Characterization of layered compounds by vibrational spectroscopy. *J. Braz. Chem. Soc.* **2006**, *17*, 1651–1657. [CrossRef]

47. Aguirre, J.M.; Gurierrez, A.; Giraldo, O. Simple Route for the synthesis of copper hydroxy salts. *J. Braz. Chem. Soc.* **2011**, *22*, 546–551. [CrossRef]

48. Švarcová, S.; Klementová, M.; Bezdička, P.; Łasocha, W.; Dušek, M.; Hradil, D. Synthesis and characterization of single crystals of the layered copper hydroxide acetate Cu$_2$(OH)$_3$(CH$_3$COO)·H$_2$O. *Cryst. Res. Technol.* **2011**, *46*, 1051–1057. [CrossRef]

49. Glugoski, L.P.; Cubas, P.J.; Fujiwara, S.T. Reactive Black 5 dye degradation using filters of smuggled cigarette modified with Fe^{3+}. *Envion. Sci. Pollut. Res.* **2017**, *24*, 6143–6150. [CrossRef]

50. Adachi, A.; Ouadrhiri, F.E.; Kara, M.; Manssouri, I.E.; Assouguem, A.; Almutairi, M.H.; Bayram, R.; Mohamed, H.R.H.; Peluso, I.; Eloutassi, N.; et al. Decolorization and degradation of methyl orange azo dye in aqueous solution by the electro fenton process: Application of optimization. *Catalysts* **2022**, *12*, 665. [CrossRef]